J. Biochem. 125, 285-296 (1999)

Mechanism for the Recognition and Activation of Substrate in Medium-Chain Acyl-CoA Dehydrogenase[1]

Haruhiko Tamaoki,* Yasuzo Nishina,† Kiyoshi Shiga,† and Retsu Miura*,[2]

*Departments of *Biochemistry and †Physiology, Kumamoto University School of Medicine, 2-2-1 Honjo, Kumamoto 860-0811*

Received September 28, 1998; accepted October 20, 1998

The mechanism underlying the recognition and activation of the substrate for medium-chain acyl-CoA dehydrogenase (MCAD) was spectroscopically investigated using 3-thia-acyl-CoAs as substrate analogs. The complex of MCAD with 3-thiaoctanoyl-CoA (3-thia-C8-CoA) exhibited a charge-transfer (CT) band with a molar extinction coefficient of $\varepsilon_{808} = 9.1\ mM^{-1} \cdot cm^{-1}$. With increasing 3-thiaacyl-chain length, the CT-band intensity of the complex decreased concomitantly with changes in the FAD absorption at 416 and 482 nm, and no CT band was detected in complexes with chain-lengths longer than C15. Detailed analysis of the absorption spectra suggested that the complexed states represent a two-state equilibrium between the CT-inducing form and the CT-non-inducing form. ^{13}C-NMR measurements with ^{13}C-labeled ligand clarified that 3-thia-C8-CoA is complexed to MCAD in an anionic form with signals detected at 163.7 and 101.2 ppm for $^{13}C(1)$ and $^{13}C(2)$, respectively. In the MCAD complex with $^{13}C(1)$-labeled 3-thia-C12-CoA, two signals for the bound ligand were observed at 163.7 and 198.3 ppm, and assigned to the anionic and neutral forms, respectively. Only the neutral form signal was measured at 200.6 ppm in the complex with $^{13}C(1)$-labeled 3-thia-C17-CoA. These results indicate that the CT band can be explained in terms of an internal equilibrium between anionic (CT-inducing) and neutral (CT-non-inducing) forms of the bound ligand. Resonance Raman spectra of the MCAD·3-thia-C8-CoA complex, with excitation at the CT band, showed enhanced bands, among which the 854- and 1,368-cm^{-1} bands were assigned to the S-C(2) stretching mode of the ligand and to flavin band VII, respectively. Since the enhanced bands were observed at the same wave numbers in complexes with C8, C12, and C14-ligands, it appears that the CT-inducing form shares a common alignment relative to oxidized flavin irrespective of differences in the acyl-chain length. However, with longer ligands, the degree of resonance enhancement of the Raman bands decreased in parallel with the CT-band intensity; this is compatible with the increase in the CT-non-inducing form in complexes with longer ligands. Furthermore, the pH dependence of the CT band gave an apparent $pK_a = 5.6$-5.7 for ligands with chain-lengths of C8-C12. The NMR measurements revealed that, like chain-length dependence, the pH dependence can be explained by a two-state equilibrium derived from the protonation/deprotonation of the CT-inducing form of the bound ligand. On the basis of these results we have established a novel model to explain the mechanism of recognition and activation of the substrates/ligands by MCAD.

Key words: acyl-CoA dehydrogenase, charge-transfer interaction, flavoenzyme, nuclear magnetic resonance, resonance Raman spectra.

[1] This work was supported by Grants-in-Aid for Scientific Research (No. 10780370, No. 07458160, and No. 10146103) and a Grant-in-Aid for Scientific Research on Priority Areas (A) (No. 10146103) from the Ministry of Education, Science, Sports and Culture of Japan and by a Research Grant from the Japan Society for the Promotion of Science (Research for the Future).

[2] To whom correspondence should be addressed. Tel: +81-96-373-5062, Fax: +81-96-372-6140, E-mail: miura@gpo.kumamoto-u.ac.jp

Abbreviations: ACD, acyl-CoA dehydrogenase; ACO, acyl-CoA oxidase; CT, charge-transfer; MCAD, medium-chain acyl-CoA dehydrogenase; 3-thia-Cn-CoA, straight-chain 3-thiaacyl-CoA, where n denotes the total number of carbon and sulfur atoms in the 3-thiaacyl-chain.

© 1999 by The Japanese Biochemical Society.

Mitochondrial acyl-CoA dehydrogenases (ACDs) are well-known flavodehydrogenases and catalyze the dehydrogenation of acyl-CoA thioesters to the corresponding *trans*-2-enoyl-CoAs (*1-3*). ACDs isolated from several mammalian species are classified into four straight-chain (short-, medium-, long-, and very long-chain) ACDs and three branched-chain (isovaleryl-, 2-methylbutyryl-, and glutaryl-CoA) dehydrogenases according to substrate specificity (*4*). Among them, porcine medium-chain ACD (MCAD), which favorably catalyzes substrates with acyl-chain lengths of C8-C10, is one of the most extensively investigated. The reaction mechanism has been shown to involve the abstraction of the *pro-R* α-proton by a catalytic base in concert with *pro-R* β-hydride transfer to FAD (*5*).

Downloaded from http://jb.oxfordjournals.org/ at Changhua Christian Hospital on October 1, 2012

The crystal structure of the complex with octanoyl-CoA (*6*) provides a mechanistic view of the activation and recognition of the substrate in the active site cavity (Scheme 1). Reaction intermediates of MCAD with suitable substrates are spectroscopically characterized by a decrease in FAD absorption at 450 nm as well as by the appearance of a long-wavelength absorption centered at around 560 nm (*7*). That the long-wavelength absorption is derived from a charge-transfer (CT) interaction between reduced FAD and the product enoyl-CoA (*7*) was fully confirmed by resonance Raman spectroscopy (*8*). On the other hand, intermediates formed with less favored substrates diminish the spectral changes derived from the generation of reduced FAD and product. The intensity of the CT band is reported to be related to the kinetic parameter V_{max} with respect to the chain-length of the substrate (*9*).

It is well known that certain types of ligands or substrate analogs show CT interactions, and the CT bands induced by these ligands have been the subjects of extensive spectroscopic investigation. Thorpe and his coworkers have studied the spectral changes with reference to the chain-length dependence of the substrate analogs, *e.g.* 3-ketoacyl-CoA and 3-thiaacyl-CoAs (*10, 11*). The CT-band strengths induced by the ligands were similarly related to the specific activities of the substrates with corresponding chain-lengths. A parallel relationship between the enzymatic properties of the substrate and ligand can be explained by the reasonable assumption that the abstraction of the α-proton is a common step in the catalytic event involving substrates and ligands as shown in Scheme 1. The degree of α-proton abstraction seems to vary according to the acyl-chain length of the substrate or ligand. As discussed previously (*12*), the introduction of multiple states of the complex, *i.e.* the equilibrium between the CT-inducing and CT-non-inducing states, provides a reasonable interpretation for the chain-length-dependent behavior of the enzyme complex with substrate or ligand.

To approach the inherent nature of MCAD with respect to substrate recognition, we studied complexes between MCAD and 3-thiaacyl-CoAs by NMR and resonance Raman spectroscopy. Resonance Raman spectroscopy with excitation at the CT band was used to detect molecular vibrations of the moiety participating in the CT interaction. Since resonance enhancements of the Raman bands reflect the alignment between the CT counterparts, spectral comparison among complexes with different ligands yields valuable information about the CT-interaction mode. NMR spectroscopy generally allows the direct detection of ^{13}C-labeled ligands in all complexed states of the ligand, and the observed signals reveal the ionization states and multiplicity of the complexed states. The combination of absorption, resonance Raman, and NMR spectroscopic data reveals the overall behavior of the MCAD complex with 3-thiaacyl-CoA in relation to 3-thiaacyl-chain length. Furthermore, the spectral investigation was extended to the pH-dependent features of the complex to clarify the linear relationship between CT-band intensity and deprotonation from the bound ligand. On the basis of the results obtained, as well as previously reported data on MCAD, we propose a plausible model for the mechanism of the substrate/ligand recognition and substrate activation.

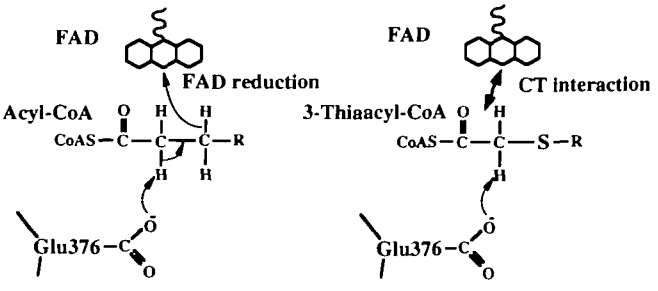

Scheme 1. **Mechanism of the activation of substrate and ligand in MCAD.**

MATERIALS AND METHODS

Preparation of MCAD and 3-Thiaacyl-CoAs—MCAD was purified from porcine kidney as described elsewhere (*13, 14*). The concentration of porcine MCAD was estimated spectrophotometrically using $\varepsilon_{446} = 15.4\ mM^{-1} \cdot cm^{-1}$ (*15*). 3-Thiacarboxylic acids were synthesized according to Uyeda and Reid (*16*). 3-Thiaacyl-CoAs were synthesized from the corresponding 3-thiacarboxylic acids by the method of Kawaguchi *et al.* (*17*). The isotopically-labeled 3-thiaacyl-CoAs were synthesized from chloroacetic acid labeled with ^{13}C at carbon-1 or -2 (99.6 or 99.7 atom% enriched, respectively, Isotec, USA). The final products were purified by reversed-phase HPLC on a C4 column (Cosmosil) eluted with a linear methanol gradient in 10 mM ammonium acetate, pH 5.3. Eluates containing the products were desalted by passage through a Sephadex G-10 column in water. All products were stored as lyophilized powder at −20°C. Mass spectra of the purified products were measured with a matrix of sinapinic acid on a Kompact MALDI III (Shimadzu/Kratos) spectrometer. The observed molecular mass of each product was identical to the value calculated from its molecular formula within an accuracy of 0.7 mass unit. 3-Thiaacyl-CoA concentrations were determined from the molar extinction coefficient of 16 $mM^{-1} \cdot cm^{-1}$ (*18*).

Preparation of MCAD Complexes—For the measurement of the absorption, Raman, and NMR spectra, the MCAD solutions were applied to a Sephadex G-50 column equilibrated with the desired buffer. The eluted solutions were used after concentration through an ultra filtration membrane, Centricon 30 (Amicon). The pH of each solution was measured by a microelectrode (Horiba) before and after measurement.

Spectroscopic Measurements—Absorption spectra were recorded with a Hitachi U-3210 spectrometer equipped with a thermostatted cell holder. Measurements of resonance Raman spectra were performed at an excitation wavelength of 632.8 nm using a He-Ne Laser (NEC GLG5900) on a JASCO NR-1800 spectrometer. ^{13}C-NMR spectra were measured with a Varian Unity-Plus 500 (operating at a ^{13}C frequency of 125.7 MHz) spectrometer with a pulse width of 30 degrees and a relaxation delay of 4 s. Each sample contained 10% D_2O for field locking and the chemical shift was externally referenced to sodium trimethyl(silyl)propanoate-d_4. The spectra were obtained by applying the Fourier transformation with a line broadening factor of 20 Hz. All spectroscopic measurements were carried out at 25°C unless otherwise specified.

Downloaded from http://jb.oxfordjournals.org/ at Changhua Christian Hospital on October 1, 2012

RESULTS

Dependence of the CT-Band Intensity of MCAD·3-Thiaacyl-CoA Complexes on the Acyl-Chain Length—Figure 1A shows the absorption spectra of MCAD and its complexes with 3-thiaacyl-CoAs with various acyl-chain lengths. In the MCAD complex, the new long-wavelength absorption band centered at 808 nm, *i.e.* the CT band, can be ascribed to the CT interaction between an anionic ligand and the oxidized form of FAD (*11*). Of the ligands used here, 3-thia-C8-CoA yielded the greatest CT-band intensity. With longer 3-thiaacyl-CoAs, the CT band intensity decreased with a drastic decrease observed between complexes with acyl-chain lengths of C11 and C12. No CT band was detected in the MCAD complex with 3-thia-C15-CoA. Similar observations concerning the chain-length dependence of the CT band have been reported by Lau *et al.* (*11*). The difference spectra of the complexes, where the MCAD·3-thia-C21-CoA spectrum is subtracted from each spectrum, show significant changes in flavin absorption at 416 and 482 nm in addition to the appearance of the CT band centered at 808 nm (Fig. 1, B and C). These spectral changes are unique in that the spectral changes are identical, although with different intensities, regardless of the acyl-chain length of the ligand. All the spectra are reminiscent of a two-state equilibrium as characterized by four isosbestic points. A similar two-state equilibrium with regard to acyl-chain length has been observed for the complexes of acyl-CoA oxidase with 3-ketoacyl-CoAs (*12*), where one of the species in the two-state equilibrium is a CT-inducing species, the other species inevitably being a CT-non-inducing species. Here, an identical CT-interaction mode is shared by complexes with CT bands; the equivalency of the CT interactions will be demonstrated later by similar resonance enhanced Raman bands observed by excitation at the CT band for the C8, C12, and C14 complexes. These chain-length-dependent spectral changes resemble changes observed at different pHs as shown in Fig. 5. However, it should be noted that the chain-length-dependent two-state equilibrium provides a correlation among the spectral behaviors observed with individual ligands and permits a generalized discussion of ligand recognition and substrate activation.

Assignment of the ^{13}C-NMR Signals of 3-Thia-C8-CoA in Complex with MCAD—To identify the state of the ligand in complex with MCAD, we measured ^{13}C-NMR spectra of MCAD complexes with ^{13}C(1)- and ^{13}C(2)-labeled 3-thia-C8-CoA (Fig. 2). The ^{13}C(2) signal at 101.2 ppm of the bound 3-thia-C8-CoA decreased with increases in the amount of non-labeled C8 ligand added, indicating that the ligand binds to MCAD reversibly. With high concentrations of non-labeled ligand, natural abundance signals were observed and the ^{13}C(2) signal at 101.2 ppm disappeared (Fig. 2C). The ^{13}C(1) signal of the bound ligand was observed at 163.7 ppm, as shown in Fig. 2D, judging from comparison with spectra of the complex with ^{13}C(2)-labeled ligands under the same conditions. In the spectra obtained for the two labeled ligands, signals from the free ligands were observed at 203.3 and 44.3 ppm for ^{13}C(1) and ^{13}C(2), respectively. The signals at 181.2 and 39.4 ppm derive from the corresponding fatty acids produced by hydrolysis of the ligands during measurement because the chemical shifts coincide with those of the corresponding acids and their intensities increase with longer measurements. The cause for ligand hydrolysis is unknown at present. The chemical shift difference between the free and bound ligands suggests that the ligand is converted from the neutral form to the anionic form when it is bound. The high-field shift in the ^{13}C(1) signal is derived from the increase in the electron density at the C(1) position, while the low-field shift of the ^{13}C(2) signal is consistent with a change in the orbital hybridization from sp^3 to sp^2. As discussed later, enzyme-bound 3-thia-C8-CoA was con-

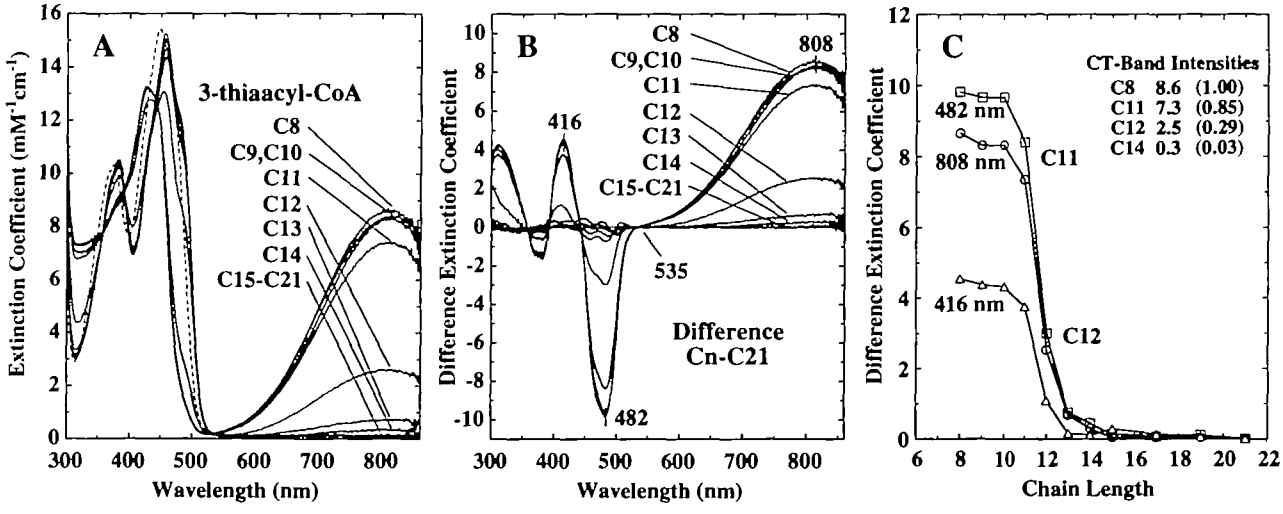

Fig. 1. **Absorption spectra of the MCAD·3-thiaacyl-CoAs complexes.** Spectra of MCAD·3-thiaacyl-CoA complexes with acyl-chain lengths from 8 to 21 (A), difference spectra between MCAD·3-thiaacyl-CoA and MCAD·3-thia-C21-CoA (B), and plots of the absorption of the difference spectra at 808, 482, and 416 nm (C). The dashed line in figure A indicates the spectrum of uncomplexed MCAD and the absorbance was scaled as the extinction coefficient on the ordinate. For each complex, a 20-fold excess of each ligand was used to saturate to the 50 μM MCAD and the absorption below 400 nm of each ligand was subtracted. Saturation was confirmed by comparing the spectra measured with a 100-fold excess of ligand. The inset in C indicates the difference extinction coefficients at 808 nm (relative values in parenthesis) estimated from figure B. All measurements were carried out in 50 mM potassium phosphate buffer, pH 7.6, at 25°C.

Downloaded from http://jb.oxfordjournals.org/ at Changhua Christian Hospital on October 1, 2012

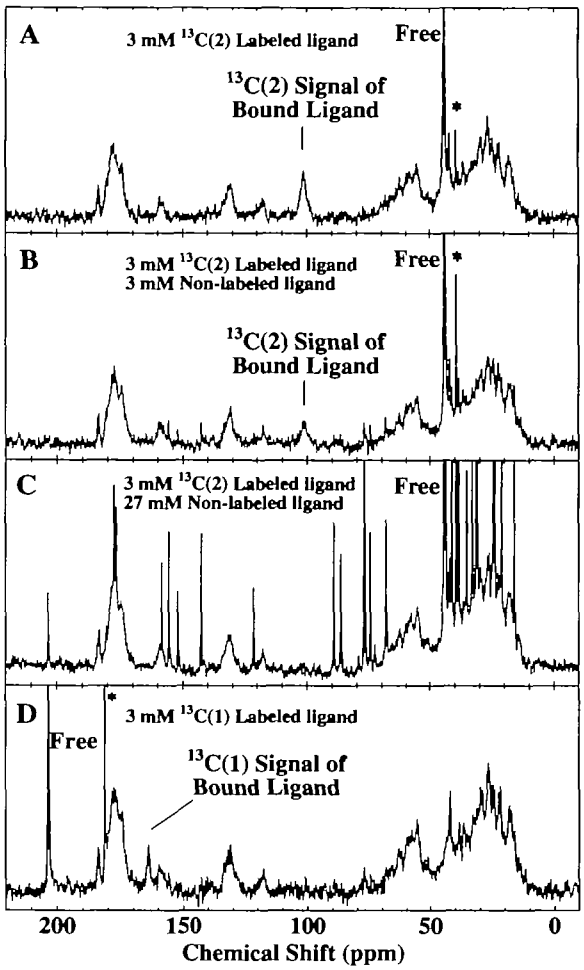

Fig. 2. **Assignment of the ^{13}C-NMR signals of enzyme-bound ligands.** NMR of the complex between 1 mM MCAD and 3 mM ^{13}C(2)-labeled 3-thia-C8-CoA (A); NMR of the complex after adding the same molar amount of non-labeled 3-thia-C8-CoA to sample A (B); and NMR after further addition of non-labeled ligand to reach a total ligand concentration of 30 mM (C). The signal of ^{13}C(2) of the ligand was assigned based on an exchange experiment of labeled ligand with non-labeled ligand (A-C) and by the comparison with the NMR spectra of a complex of 1 mM MCAD with 3 mM ^{13}C(1)-labeled 3-thia-C8-CoA (D). A signal due to free ligand was observed in each spectrum; * indicates the signal of the fatty acid by hydrolysis of the corresponding ligand. All measurements were carried out with proton decoupling in 50 mM potassium phosphate buffer, pH 7.0, at 25°C. All spectra were means for 8,000-20,000 transients.

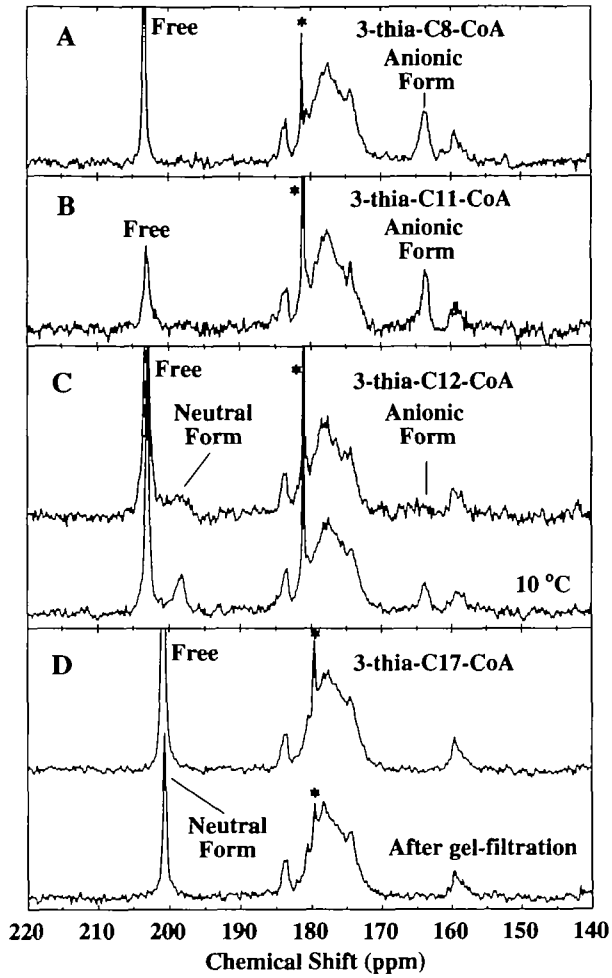

Fig. 3. **Chain-length dependence of the ^{13}C(1) signals of enzyme-bound 3-thiaacyl-CoAs.** ^{13}C-NMR spectra were measured without proton decoupling for the MCAD complex with 3-thiaacyl-CoAs with acyl-chains of C8 (A), C11 (B), C12 (C), and C17 (D) in 50 mM potassium phosphate buffer, pH 7.0. All spectra were obtained at 25°C except the lower spectrum in C (10°C). Sample concentrations were 1 and 3 mM for enzyme and ligand, respectively, for all except the lower spectrum in D. The lower spectrum in D was recorded on sample following the removal of free ligand by gel-filtration of the sample for upper spectrum of D. Measurements were continued for 20,000-40,000 transients and * indicates the signal due to fatty acid caused by the hydrolysis of the corresponding ligand.

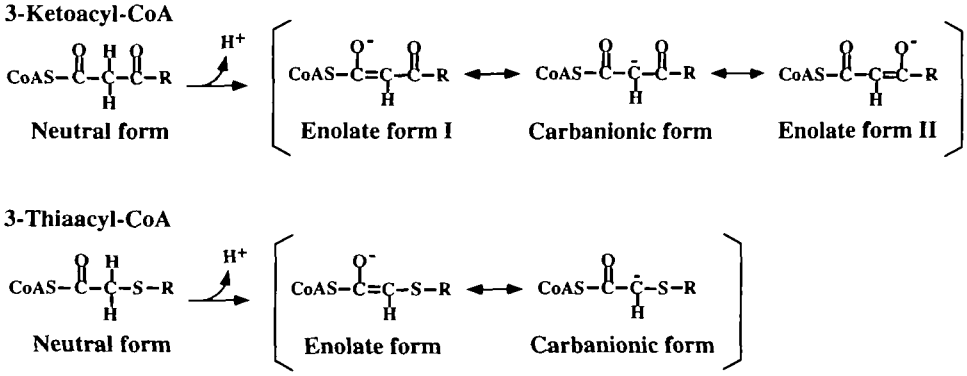

Scheme 2. **Canonical structures of anionic ligands, 3-ketoacyl-CoA and 3-thiaacyl-CoA.**

Downloaded from http://jb.oxfordjournals.org/ at Changhua Christian Hospital on October 1, 2012

firmed to exist predominantly in an anionic state (Scheme 2).

Dependence of the ^{13}C-NMR Signals of 3-Thiaacyl-CoAs Bound to MCAD on Acyl-Chain Length—NMR signals of $^{13}C(1)$-labeled ligands were measured for complexes of MCAD complexes with ligands of chain-length C8, C11, C12, and C17 (Fig. 3). The ^{13}C chemical shifts of the free and bound ligands are summarized in Table I. In MCAD complex with 3-thia-C8-CoA or 3-thia-C11-CoA, a signal from the enzyme-bound anionic ligand was observed at 163.7 ppm (Fig. 3, A and B). In contrast, the complex with 3-thia-C12-CoA produced a new signal at around 198.3 ppm that appeared concomitantly with the decrease in intensity of the signal at around 163.7 ppm (upper trace in Fig. 3C). From its chemical shift, the signal at 198.3 ppm appears to be derived from the neutral species of the bound ligand. Compared with the shape of the band at 163.7 ppm observed in the complex with 3-thia-C8-CoA, the two bands appear broadened, probably due to multiple states of the neutral or anionic bound forms. Indeed, measurement made at 10°C produced sharper band shapes (compare the two traces in Fig. 3C), probably because more stable forms predominate at lower temperatures. In the complex with excess 3-thia-C17-CoA, only one broad signal was observed at 200.8 ppm, a similar chemical shift to that of the free ligand. Removal of the excess free ligand by gel-filtration sharpened the signal at 200.6 ppm. Thus, enzyme-bound 3-thia-C17-CoA is concluded to be exclusively in the neutral form. To confirm that the signal observed at 200.6 ppm is due to the neutral bound form, ^{13}C-NMR measurement was made of the MCAD complex with 3-thia-C17-CoA labeled with ^{13}C at the C(2) carbon. The bound form was observed at 44.6 ppm as anticipated for an sp^3-carbon of the neutral form (results not shown). The signal intensity at 163.7 ppm showed a linear correlation with the corresponding CT-band strength for the complex with 3-thia-acyl-CoAs. The decrease in the signal at 163.7 ppm increased the signal assigned to the neutral form in the case of 3-thia-C12-CoA or 3-thia-C17-CoA. Therefore, the observation of two $^{13}C(1)$ signals reveals that the enzyme-bound ligands exist generally in two forms, *i.e.* neutral and anionic forms, and that the relative population of the two

TABLE I. **^{13}C chemical shifts of free and MCAD-bound 3-thiaacyl-CoAs.**

		Chemical shift (ppm)				
		Acetoacetyl-CoA[a]	3-Thia-C8-CoA	3-Thia-C11-CoA	3-Thia-C12-CoA	3-Thia-C17-CoA
$^{13}C(1)$	Free	198.5	203.3	203.1	203.1	200.8
	Bound	181.3	163.7	163.7	163.7[b], 198.3[b]	200.6[c]
$^{13}C(2)$	Free	59.9	44.3	nd	nd	44.6
	Bound	103.4	101.2	nd	nd	44.6[c]

[a]Chemical shifts are from Ref. *24*. [b]Chemical shifts were measured at 10°C. [c]Measured after gel-filtration to remove free ligand. nd: not determined.

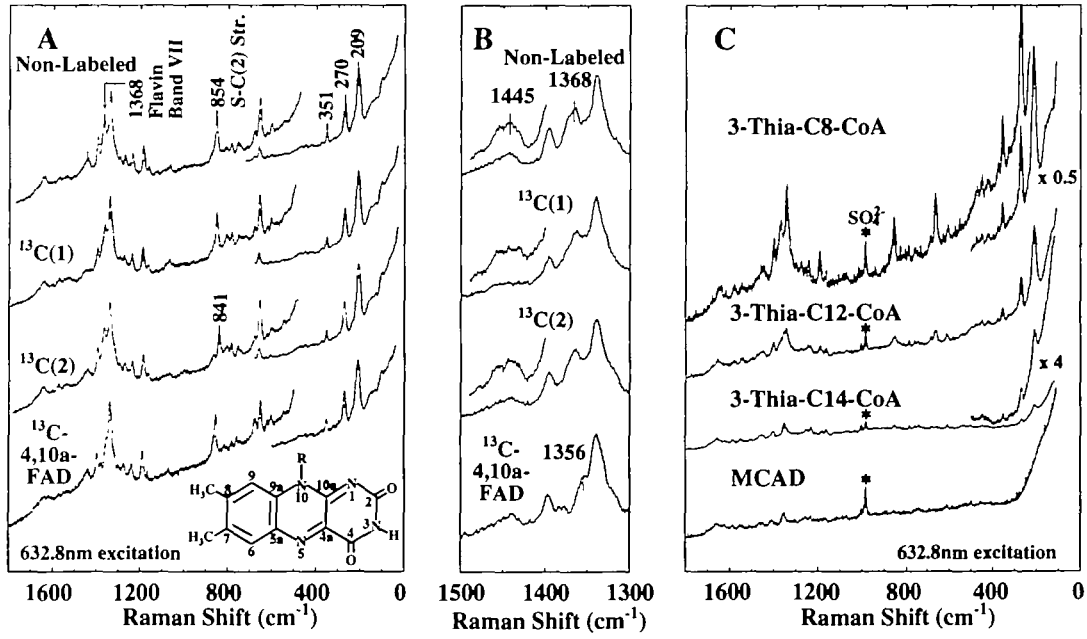

Fig. 4. **Resonance Raman spectra of MCAD·3-thiaacyl-CoAs complexes.** Some enhanced Raman bands in the MCAD·3-thia-C8-CoA complex were assigned using ^{13}C-labeled ligands or FAD (A and B). The chain-length dependence of the resonance enhancement of complexes with 3-thia-C8-CoA, 3-thia-C12-CoA, and 3-thia-C14-CoA is shown (C). All measurements were carried out in 50 mM potassium phosphate, pH 7.6, at 25°C. (A) and (B): Concentrations were 1.1 mM MCAD and 3.5 mM ligand; (C): concentrations were 1.1, 2.8, and 4.5 mM for MCAD complexes with C8, C12, and C14-ligands, respectively. Each complex was measured in the presence of 1.5–2.0-fold excess ligand. The spectrum for uncomplexed MCAD was recorded under the same conditions (1.1 mM enzyme). Preparation for Raman measurement (C) contained 1% of ammonium sulfate. The SO_4^{2-}-stretching signal at 981 cm^{-1} was used for normalization of the intensity.

Downloaded from http://jb.oxfordjournals.org/ at Changhua Christian Hospital on October 1, 2012

forms varies with the acyl-chain length of the ligand.

Resonance Raman Spectra of Complexes of MCAD with 3-Thiaacyl-CoAs—Excitation within the charge-transfer band of the complex causes certain Raman bands to exhibit resonance enhancement. Of these enhanced bands, some were assigned based on the isotope shifts of the ligand or FAD (Fig. 4A). In the complex between MCAD and $^{13}C(1)$-labeled 3-thia-C8-CoA, the spectral pattern in the range 1,300-1,500 cm^{-1} shows subtle differences compared with the complexes between MCAD and non-labeled or $^{13}C(2)$-labeled ligand (Fig. 4B). However, we were unable to identify the band for the C(1)=O [or C(1)-O^-] stretching mode in the difference spectrum between the bound forms of the $^{13}C(1)$-labeled and non-labeled ligands (data not

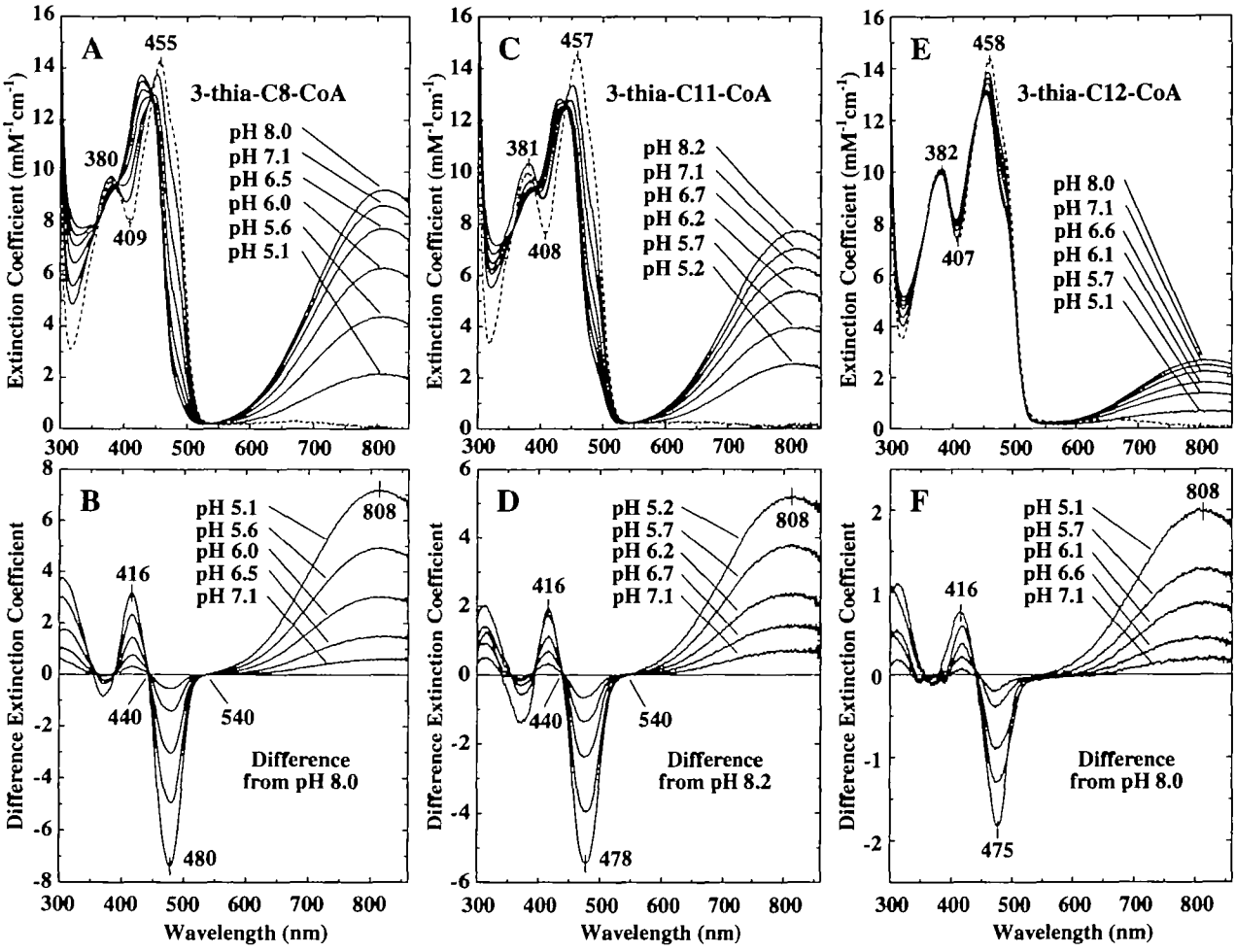

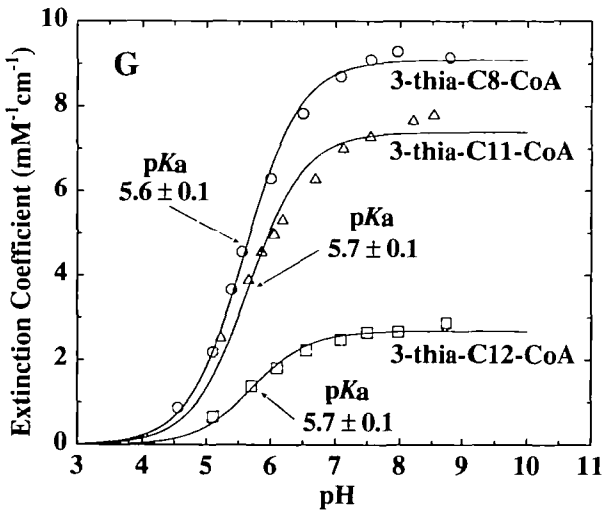

Fig. 5. **pH and chain-length dependence of the CT-band intensities of MCAD complexes with 3-thiaacyl-CoAs.** Spectra obtained at different pH are shown for complexes with 3-thia-C8-CoA, 3-thia-C11-CoA, and 3-thia-C12-CoA (A, C, and E); the dashed lines represent simulated spectra of the acidic state at low pH. B, D, and F show difference spectra (spectrum − spectrum at pH 8.0 or 8.2) to clarify the subtle differences between ligands. Three kinds of buffer were used; 50 mM sodium acetate (pH < 5.5), 50 mM potassium phosphate (pH 5.5-7.8), and 50 mM Tris-HCl (pH > 7.8). All experiments were obtained in the presence of 20-fold excess ligand at 25°C. The enzyme concentrations were in the range of 53-60 μM, and the absorbance was normalized as the extinction coefficient on the ordinate. The CT-band intensities at 808 nm were plotted for the complex with each ligand, C8 (○), C11 (△), C12 (□) (G). Solid lines in G were drawn on the basis of the two-state model. Estimated pK_a values are 5.6 ± 0.1, 5.7 ± 0.1, and 5.7 ± 0.1 for complexes with C8, C11, and C12-ligands, respectively.

Downloaded from http://jb.oxfordjournals.org/ at Changhua Christian Hospital on October 1, 2012

shown); the difference spectrum shows a weak and diffuse pattern in the range 1,300-1,450 cm^{-1} where C(1)=O or C(1)-O^- stretching is normally expected to appear. In the complex with the $^{13}C(2)$-labeled ligand, a down shift in the 854-cm^{-1} band by 13 cm^{-1} indicates that this band makes a large contribution to the S-C(2) stretching mode. Furthermore, a band from FAD was observed at 1,368 cm^{-1} that undergoes a 12 cm^{-1} down shift upon reconstitution with [^{13}C-4,10*a*]FAD. On the basis of the normal mode analysis of lumiflavin (*19, 20*), the 1,368-cm^{-1} band was assigned to flavin band VII, which is derived from the stretching modes of the C(5*a*)-C(6) and N(10)-C(10*a*) bonds. The remaining bands were insensitive to isotopic exchange by ^{13}C in the ligand or FAD. The three intense bands observed at 351, 270, and 209 cm^{-1} seem to be related to the bending mode of the isoalloxazine ring, since the corresponding frequencies were calculated in the normal mode analysis of the isoalloxazine ring (*20*). Changing the ligand to those with longer 3-thiaacyl-chains caused the intensities of the resonance enhanced Raman band to decrease (Fig. 4C) in agreement with the decrease in the CT-band intensity. However, the wave numbers of these enhanced bands were independent of the chain-length of the ligand. In particular, the wave numbers and their intensity ratios remain constant, although the intensities of the three resonance enhanced bands at 351, 270, and 209 cm^{-1} decrease in ligands with longer acyl-chains. Normalization of the band intensities to the internal reference of the SO_4^{2-}-stretching band enabled a direct comparison of the resonance enhancements of the three complexes. Based on the band intensities at 351, 270, and 209 cm^{-1}, the resonance enhancements of the three complexes were estimated to decrease with a ratio 1:0.28:0.04 according to the difference in the chain-length of ligands C8, C12, and C14, respectively. Since this ratio is similar to that of the CT-band intensities, 1:0.29:0.03 for complexes with C8, C12, and C14, respectively (values in Fig. 1C), the CT-band intensity is directly correlated with the enhancement of the Raman bands. It is also concluded that the anionic form of the ligand and oxidized FAD interact in the same charge-transfer mode in all complexes regardless of the chain-length of the ligand.

pH Dependence of the CT-Band of MCAD Complexes with 3-Thiaacyl-CoAs—As described in the preceding sections, the spectroscopic measurements revealed the presence of two forms of bound ligand at neutral pH. In this section, we demonstrate the pH dependence of the CT-band strength can be interpreted as the acid-base equilibrium between the enzyme and the ligand. Figure 5A shows the absorption spectra of the MCAD complex with 3-thia-C8-CoA at various pHs. Since all spectra correlate with four isosbestic points at 540, 440, 390, and 360 nm, the spectral behavior is consistent with a two-state model. The plot of the CT-band strength as a function of pH yields $pK_a = 5.6 \pm 0.1$ and an extrapolated maximum extinction coefficient $\varepsilon = 9.1 \pm 0.2$ $mM^{-1} \cdot cm^{-1}$ (Fig. 5G). Similar pH dependencies were observed for complexes with 3-thiaacyl-CoAs with acyl-chain lengths of C11 and C12. In other cases, despite similar apparent pK_a values, the extinction coefficients of the CT bands reached individual maximum CT intensities at higher pH. The values of the maximum extinction coefficients are in the order of their acyl-chain lengths, *i.e.* $\varepsilon_{808} = 9.1$, 7.4, and 2.7 $mM^{-1} \cdot cm^{-1}$ for chain-lengths C8, C11, and C12, respectively.

Based on the assumption that the pH dependence of the absorption spectra can be explained by a two-state acid-base model, we simulated the spectrum of the acidic state at lower pH from the spectra at pH > 5.5 by least squares treatment. The simulated spectrum, shown by the dashed line for each complex in Fig. 5, A, C, and E, was obtained with a standard deviation within 0.5 $mM^{-1} \cdot cm^{-1}$ for each complex. These three simulated spectra indicate similar patterns; however, substantial differences were noted in the wavelengths of the spectral peaks and troughs of FAD around 455, 380, and 410 nm.

To gain better insight into the origin of pH-dependent CT-band intensity, NMR measurements were applied to MCAD complexes with $^{13}C(1)$- or $^{13}C(2)$-labeled 3-thia-C8-CoA at different pHs. Figure 6 shows the decrease in the intensities of the 163.7 and 101.2 ppm peaks derived from the anionic form of the bound ligands with decreasing pH. After the measurements at pH 5.8, NMR spectra of the same enzyme solutions were obtained after changing the pH. Since the spectra obtained at pH 7.3 display similar patterns to those obtained at pH 7.0, we conclude that the pH-dependent behavior is reversible. For the absorption

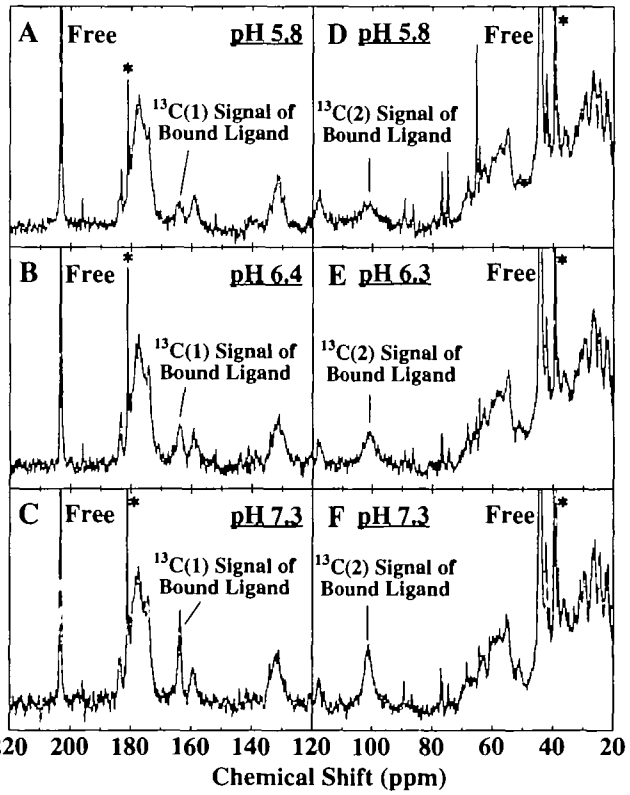

Fig. 6. **pH dependence of the ^{13}C-NMR signals of the MCAD complex with 3-thia-C8-CoA.** Spectra A-C (without proton decoupling) and D-F (with proton decoupling) were measured using $^{13}C(1)$- and $^{13}C(2)$-labeled ligands, respectively. The same enzyme sample was used repeatedly for each spectral series (A-C and D-F). Sample concentrations were 1 and 3 mM for enzyme and ligand, respectively. All measurements were carried out in 50 mM potassium phosphate buffer at 25°C. All spectra are means of 40,000 transients and * indicates the signal of the fatty acid caused by the hydrolysis of the corresponding ligand. The signal intensities of the anionic ligands observed at 163.7 and 101.2 ppm correlate with the pH dependence of the CT-band intensity shown in Fig. 5, A and G.

Downloaded from http://jb.oxfordjournals.org/ at Changhua Christian Hospital on October 1, 2012

spectra, this reversibility was confirmed by changing the pH of the solution of the MCAD complex with 3-thia-C8-CoA from 4.5 to 8.0 (data not shown). The absence of an increase in the ^{13}C signal of the neutral form is possibly due to exchange behavior derived from the combination of the on and off rates of the bound neutral form and the free ligand. A fast exchange between the bound and free ligands should result in an averaging of the two chemical shifts. In this context, in the complex of enoyl-CoA hydratase with cinnamoyl-CoA, the addition of excess ligand resulted in a shift of the broad signal assigned to the bound ligand without the appearance of the new signal expected for the free ligand (*21*). Further studies are needed to reach a final conclusion in the present case.

DISCUSSION

Complexes of MCAD with several classes of substrates and ligands have been studied both thermodynamically and kinetically in order to understand the mechanisms underlying the recognition and activation of substrates (*10, 22*). In complexes with 3-ketoacyl-CoAs, the CT interaction, which induces an absorption band at about 550 nm, was investigated by absorption (*10*), resonance Raman (*8, 23*), and ^{13}C-NMR (*24*) spectroscopy. The band was demonstrated to derive from the charge-transfer interaction between the anionic ligand and oxidized flavin. These spectral observations imply that the enzyme-bound form of the ligand is anionic and stabilized by the resonance of three canonical structures (Scheme 2). The C(3)=O group participates in the delocalization of the negative charge produced by α-proton abstraction; the site of delocalization extends from C(1)-O^- to C(3)-O^-. Since the delocalization site does not involve S(3) in the case of the anionic form of 3-thiaacyl-CoAs, the anionic form is expected to make a relatively large contribution to a canonical form of enolate -C(2)=C(1)-O^-, as compared to 3-ketoacyl-CoAs. The differences in the resonance structures are reflected in the ^{13}C-NMR resonance position of the $^{13}C(1)$ signal. The localization of a negative charge at the enolate oxygen results in a high-field shift of 39.6 ppm at the $^{13}C(1)$ signal from the free ligand (Table I), while the corresponding shift in 3-ketoacyl-CoA is only half as much, *i.e.* 17.2 ppm (*24*). Conversely, the low-field shift in the $^{13}C(2)$ signal seems to arise primarily from the change in hybridization from sp^3 to sp^2 at C(2). In fact, the $^{13}C(2)$ signals of the anionic form were observed to have similar chemical shifts, *i.e.* 101.2 and 103.4 ppm for 3-thiaacyl-CoA and 3-ketoacyl-CoA, respectively, despite a larger chemical shift difference between the two free ligands (44.3 and 59.9 ppm, respectively). Thus, we can not estimate the contribution of the canonical form of carbanion -C(2)$^-$-C(1)=O based on the chemical shift values of the $^{13}C(2)$ signals.

Lau *et al.* (*11*) reported a correlation between chain-length dependence of the CT-band strength of ligands and the catalytic activity of the substrates. However, the origin of the acyl-chain length dependence was unclear in their report since the bound forms of the ligands had not been unequivocally identified. In the present work, we measured the ^{13}C-NMR spectra of 3-thiaacyl-CoAs bound to MCAD, and succeeded in identifying two forms of the bound ligand, *i.e.* an anionic form and a neutral form. As shown in Fig. 3, the intensity of the signal due to the anionic form of the bound ligand decreases as the chain-length of the ligands increases from C8 to longer acyl-chains, and the signal corresponding to the anionic form is completely missing in the C17 derivative. The critical change in the signal intensity of the anionic form occurs between chain-lengths C11 and C12; this change is consistent with changes observed in the absorption spectra as shown in Fig. 1. The ratio of the two forms varies depending on acyl-chain length; in the case of 3-thia-C8-CoA, the most favorable ligand, the equilibrium is shifted far to the anionic form, while in the case of other less favorable ligands the equilibrium is shifted more to the neutral form; the equilibrium in the C17 derivative is almost exclusively in the neutral state. The fact that the relative activities of the substrates exhibit a similar chain-length dependence as seen for spectral changes in the complex with ligands can be explained by the degree of α-proton abstraction, which is shared equally during the catalytic event by a substrate and ligand. That is, in the case of a favorable substrate, the equilibrium of the two-state is directed to the formation of the product initiated by α-proton abstraction of the substrate. A similar feature of the spectral changes was observed for the complex between acyl-CoA oxidase and 3-ketoacyl-CoAs, and we postulated a similar two-state model for the bound ligands, *i.e.* an "active" form (a productive binding mode) and an "inactive" form (an abortive binding mode) (*12*). Thus, our previous hypothesis was experimentally confirmed in MCAD, which belongs to the same family as acyl-CoA oxidase (*4*). The productive binding mode provides a CT-inducing complex in contrast to the abortive binding mode as shown in Fig. 7. The ratio of the two modes is in internal equilibrium (K_{int}) when the ligand is bound to the enzyme. The generation of the two binding modes seems to result from a conformational change in the enzyme, as discussed below, that is induced by the interaction between the acyl-chain of the ligand and the active site cavity of the enzyme.

Excitation at the CT-absorption band induces resonance enhancements of the Raman bands of the vibrational modes that include molecular motions of the moieties participating in the CT interaction. In the MCAD·3-thia-C8-CoA complex, resonance Raman spectra were observed in the range of 1,800-100 cm^{-1}. The 1,368-cm^{-1} band was assigned to band VII of flavin, *i.e.* the stretching band of the C(5a)-C(6) and N(10)-C(10a) bonds, and the 854-cm^{-1} band to the stretching of the S-C(2) bond of the ligand. Most of the prominent bands were detected at the lower wave numbers of 351, 270, and 209 cm^{-1}, although their assignments await further studies. These three bands were insensitive to the ^{13}C isotopic label of the ligand at C(1) or C(2). In complexes with 3-thia-C12 and 3-thia-C14, the three bands were also observed without any band shifts. With regard to chain-length dependence, it is notable that the degree of resonance enhancement of the three bands is parallel to the individual intensities of the CT bands of the complexes (Figs. 1C and 4C). The coincidence observed in the Raman and absorption spectra supports the notion that the CT complexes share a common interaction mode between the anionic ligand and the oxidized flavin regardless of the 3-thiaacyl-chain length. The decrease in band enhancements in complexes with longer 3-thiaacyl-chains can be explained by the decrease in the CT complex as the result of an increase in the non-CT complex. Similar

Downloaded from http://jb.oxfordjournals.org/ at Changhua Christian Hospital on October 1, 2012

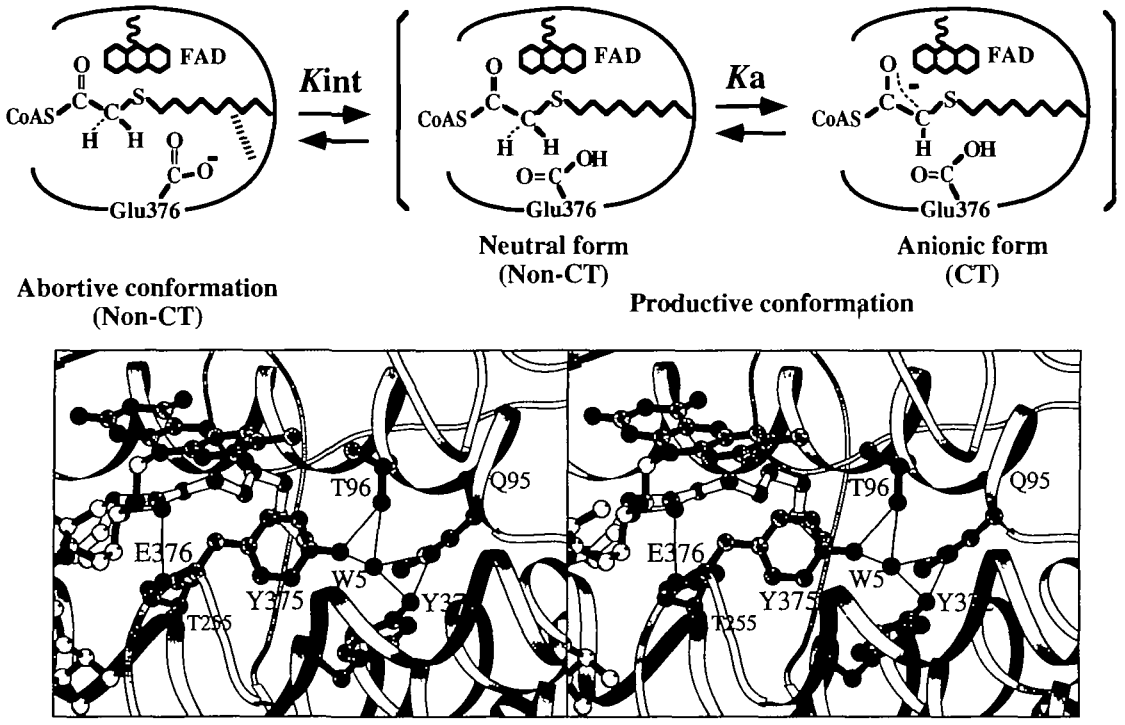

Fig. 7. **Model for substrate/ligand recognition and activation of MCAD.** The upper panel depicts the pH and chain-length dependence of the MCAD complex with substrate or ligand. K_{int} represents the equilibrium constant between the productive and abortive conformations. K_a is the apparent equilibrium constant between the anionic and neutral ligand forms in the productive conformation. The lower panel shows the active site structure of MCAD. The stereoview of the tertiary structure was drawn based on the coordinates of the MCAD•octanoyl-CoA complex (*6*) (chain A of 3MDE in PDB) with the MOLSCRIPT program (*36*). FAD, octanoyl-CoA, and the residues related to hydrogen bonding are depicted with a ball-and-stick model. W5 indicates bound water, which also participates in the hydrogen-bonding network at the bottom of the active site cavity. Note that W5 is absent in the homo-domain formed by chain B. Solid lines show hydrogen bonds as estimated by the HBPLUS program (*37*).

insensitivity of the resonance Raman band positions to ligand chain-length was reported for MCAD•3-kotoacyl-CoA complexes (*23*). Although the extent of the band enhancements was not determined, identical spectral features were shared by complexes with 3-ketoacyl-chain of C5–C16 in the region of 1,700–1,400 cm^{-1}, in which the prominent bands were assigned to the stretching band of C(4*a*)-N(5) of flavin, and to the stretching bands of C(1)=O and C(3)=O of the ligand (*23*). The stabilization induced by the CT interaction should play a significant role in fixing the configuration between the anionic ligand and the oxidized flavin ring. Resonance Raman spectroscopic studies on the MCAD complex with the ligands (3-keto and 3-thiaacyl-CoAs) provide additional evidence for the two-state equilibrium between the CT-inducing complex and CT-non-inducing complex.

The tertiary structures of the MCAD complexes with acyl-CoAs with different chain-lengths suggest that the favorability of the substrate to MCAD is determined by the hydrogen-bonding network located at the bottom of the active site cavity (*25, 26*). When the chain-length of the substrate is long enough to reach the bottom of the active site cavity, the hydrogen-bonding network would be broken by the terminal acyl-chain or the ω-end of the acyl-chain would be turned back. This interpretation is compatible with the change in the equilibrium between the two species with chain-length dependence. On the basis of the crystal structure of the MCAD•C8-CoA complex (*6*), we depict the hydrogen-bonding network at the bottom of the active site cavity (Fig. 7). One (W5) of the water molecules found in the active site cavity of the substrate-free enzyme remains in the MCAD•C8-CoA complex tightly hydrogen-bonded to the hydroxyl groups of Tyr372 and Tyr375, and the γ-amide group of Gln95 (*6*). The hydroxyl group of Tyr375, which neighbors the catalytic base Glu376, also participates in the hydrogen-bonding network at the bottom of the site. In addition, the carbonyl oxygen of the thioester is hydrogen-bonded to the ribityl 2′-hydroxyl group of FAD and the amide nitrogen of Glu376. The two hydrogen bonds are responsible for substrate activation by reducing the pK_a value through polarization of the carbonyl oxygen. Ghisla *et al.* (*27*) confirmed that hydrogen bonding to the ribityl 2′-hydroxyl group crucially reduces the pK_a value of the substrate by comparing the reactivity of the normal enzyme with the enzyme reconstituted with ribityl 2′-deoxy-FAD. In the case of the ligand, the two hydrogen bonds observed in the complex MCAD•C8-CoA are also expected to contribute to reducing the pK_a value of the ligand. In fact, the pK_a for the α-methylene proton of the enzyme-bound 3-thiaacyl-CoA was observed to be 5.6–5.7 (Figs. 5 and 7), which indicates a drastic decrease from the pK_a value of 15–16 estimated for free 3-thiaacyl-CoA (*11, 28*). Once the hydrogen-bonding network at the bottom of the cavity is broken by interaction with the longer acyl-chain, its influence is assumed to be propagated to the reaction center around the catalytic base to induce the rearrange-

Downloaded from http://jb.oxfordjournals.org/ at Changhua Christian Hospital on October 1, 2012

ment of the spatial configuration. Based on the above assumption, the two events, one at the bottom and the other at the reaction center of the active site cavity, should be linked to each other. The view of the active site cavity (Fig. 7) suggests that the phenolic ring of Tyr375 is located at a key position for linking the two events. Polarization by hydrogen bonding at the carbonyl oxygen is expected to induce a low-field shift in the chemical shift of the $^{13}C(1)$ signal, as reported for the complex of enoyl-CoA hydratase with cinnamoyl-CoA (*21*). However, in our experiment, the $^{13}C(1)$ signals observed at 198.3 and 200.6 ppm for the complexes with C12 and C17 ligands, respectively, indicate a high-field shift in comparison with the corresponding free ligands. This supports the conclusion that the abortive conformation is concurrent with breaking hydrogen bonding to the carbonyl group of the ligand.

The two-state model proposed here can be extended to interpret the pH dependence of CT-band strength. Figure 5 shows that ligands with different chain-lengths have almost the same apparent pK_a values, 5.6-5.7, implying that the acid-base process between the catalytic base and ligand proceeds similarly regardless of the chain-length. For each ligand, the CT band reaches a maximum of different intensity at higher pH (Fig. 5G). It is especially notable that there is a large gap in the CT-band intensity between chain-lengths of C11 and C12. ^{13}C-NMR measurement confirmed that the decrease in the CT band at low pH is the result in a population decrease in the anionic bound form (Fig. 6). According to the two-state equilibrium observed for both chain-length and pH dependency, we propose the novel model shown in Fig. 7. This model relies on the assumption that the equilibrium between the productive and abortive conformations is not influenced by pH. Thus, the apparent pK_a values are the same for MCAD complexes with 3-thia-C8, C11, and C12-CoA despite differences in the maximum CT intensity. The multiple conformations of the double mutant of human MCAD (Glu376Gly/Thr255Glu) (*29*) would be consistent with the existence of a productive ("active") alignment and an abortive ("inactive") alignment. In the case of the mutant enzyme, the "inactive" alignment results from the formation of a hydrogen bond at the glutamate residue which would otherwise be responsible for the abstraction of the α-proton from the substrate.

The two-state model is still valid for the "purple" complex between the reduced form of MCAD and the product. The resonance Raman spectra of the MCAD "purple" complex produced upon reaction with C4-C16-CoAs showed very similar spectral patterns with the C(1)=O stretching band of 2-enoyl-CoA appearing at 1,577 cm^{-1} (*8, 30*). In this case, reduced flavin acts as the charge-donor and 2-enoyl-CoA as the charge-acceptor in the CT interaction. This demonstrates that the same mode of CT interaction is shared by all the complexes examined. The CT band centered at 580 nm, which varies in intensity depending on the chain-length of the substrate, shows a good correlation with the corresponding turnover number (*9*). The chain-length dependence of the CT band in the MCAD·acyl-CoA complex is similar to that observed for complexes with both ligand series, *e.g.* 3-thiaacyl-CoAs and 3-ketoacyl-CoAs. The coincidence observed in the chain-length dependence of the ligands and substrate seems to reconcile the common mechanism discussed above. Since the abstraction of the substrate α-proton is concerted with the β-hydride transfer to flavin (*5*), only the productive conformation in Fig. 7 allows the reductive half-reaction with the substrate. The abortive conformation generated by the interaction with longer acyl-chains remains complexed with the substrate acyl-CoA, which is not converted to 2-enoyl-CoA. The existence of a two-state equilibrium depending on the acyl- chain length was also observed for the mutant enzyme, human MCAD (Glu376Gly/Thr255-Glu) (Fig. 3 of Ref. *31*).

Recently, Vock *et al.* (*28*) reported the pH dependency of the CT band of the complex between recombinant human MCAD and 3-thia-C8-CoA with an apparent $pK_a \approx 5.2$. The Dixon plot of the binding constants yielded pK_a values for the ligand·Glu376 moiety in the complexed enzyme and Glu376 in the free enzyme of about 5.25 and 6.3, respectively. Their experiment demonstrated that the pH-dependent behavior of the CT band can be interpreted as reflecting the acid-base reaction between the α-methylene group of the ligand and the catalytic base Glu376. The microscopic pK_a of the catalytic base in the free enzyme was shown to be similar, 6.2, as determined by the microcalorimetric titration of octenoyl-CoA to pig MCAD (*32*). In the case of enoyl-CoA, the reaction product, only the catalytic base is responsible for the pH dependence of the binding constant because the α-proton in the product is unavailable. In experiments with the product, the MCAD complex with 4-thiaenoyl-CoA revealed pH-dependent spectral changes that were interpreted by the two-state equilibrium as derived from the difference in the polarization states of the bound ligand, *i.e.* the unpolarized and polarized forms (*10, 33*). The pH dependence of ligand polarization is expected to reflect ionization of the catalytic base Glu376 and to provide the apparent pK_a value, since 4-thiaenoyl-CoA is polarized in the complex in a pH-independent manner with the mutant enzyme Glu376Gln. Unlike in our experiments, the apparent pK_a value of the MCAD·4-thiaenoyl-CoA was found to be chain-length dependent. Rudik *et al.* (*33*) suggested that the chain-length dependence of the pK_a values results from the difference in active-site desolvation by the ligand. Greater desolvation by the favorable chain-length (C8) results in the maximum pK_a value of 9.2-9.3, while the poorer match between the enzyme cavity and ligands with longer chains produces weaker desolvation and correspondingly lower pK_a values. In this case, however, the bridging mechanism between the polarization of 4-thiaenoyl-CoA and the protonation of Glu376 is unclear (*33*), and a longer product decreases the extent of maximum polarization in comparison with the C8-product (*10*). Unfortunately, our experiments did not allow us to detect the ionization of the catalytic base Glu376. In the abortive conformation of the MCAD complex with the longer 3-thiaacyl-chain, the ionization state of Glu376 is unclear. However, in the productive conformation, Glu376, which is responsible for the abstraction of the α-proton, is thought to be in the protonated carboxylic form over the pH range investigated. Since the ionization depends on the electrostatic potentials of the charge states of other charged groups (*34*), the energetic disadvantage resulting from a negatively-charged glutamate residue neighboring the anionic ligand at higher pH is thought to increase the microscopic pK_a value of the glutamate residue in the hydrophobic active site cavity.

Downloaded from http://jb.oxfordjournals.org/ at Changhua Christian Hospital on October 1, 2012

The common apparent $pK_a = 5.6$–5.7 observed for complexes with 3-thiaacyl-CoAs results from the common microscopic pK_a values of the ligands regardless of the 3-thiaacyl-chain length. The difference in the chain-length dependence of pK_a observed by Rudik *et al.* and us may be due to the different types of ligands used or to a difference in the ionization state of Glu376. To clarify this, the origin of the polarization in the complex with 4-thiaenoyl-CoA as well as the ionization state of the catalytic base in complexes with 3-thiaacyl-CoAs need to be confirmed. The construction of a mechanistic model including the deprotonation of Glu376 awaits further knowledge about ligand polarization.

We have used spectroscopy to determine the species of 3-thiaacyl-CoAs bound to MCAD, *i.e.* the anionic or neutral form in a two-state equilibrium. The population of the anionic form as detected by NMR provides a reasonable interpretation for the pH and chain-length dependencies of the CT-band strength. If the complex exists in a single conformation, then the variation in the CT-band intensities can be interpreted as due to differences in alignment between the ligand and the oxidized flavin. In fact, in mutant MCAD Glu376Asp, the lowest-energy configuration between the ligand and oxidized flavin successfully explains the spectral and energetic observations for complexes with octenoyl-CoA, acetoacetyl-CoA, and *trans*-3-indoleacryloyl-CoA (*35*). In our case, however, NMR measurements of MCAD•3-thiaacyl-CoA complexes prove the existence of two bound forms of the ligand and lead us to propose a novel model. On the basis of this acid-base model, all known complexes between MCAD and various kinds of ligands and substrates can be easily understood. However, the rationale for the internal equilibrium of the two forms of the ligand remains unknown. Further investigations of conformational aspects of the enzyme are needed to solve this issue. Crystallographic demonstration of the two forms, abortive and productive, would directly prove our two-state model.

The authors thank Dr. K. Sato of Kumamoto University School of Medicine for stimulating discussion of our proposed model.

REFERENCES

1. Beinert, H. (1963) Acyl coenzyme A dehydrogenase in *The Enzymes* 2nd ed. (Boyer, P.D., Lardy, H., and Myrbäck, K., eds.) Vol. 7, pp. 447–466, Academic Press, New York
2. Schulz, H. (1991) Beta oxidation of fatty acids. *Biochim. Biophys. Acta* **1081**, 109–120
3. Kunau, W.-H., Dommes, V., and Schulz, H. (1995) β-Oxidation of fatty acids in mitochondria, peroxisomes, and bacteria: A century of continued progress. *Prog. Lipid Res.* **34**, 267–342
4. Tanaka, K. and Indo, Y. (1992) Evolution of the acyl-CoA dehydrogenase/oxidase superfamily in *New Developments in Fatty Acid Oxidation* (Coates, P.M. and Tanaka, K., eds.) pp. 95–110, Wiley-Liss, New York
5. Pohl, B., Raichle, T., and Ghisla, S. (1986) Studies on the reaction mechanism of general acyl-CoA dehydrogenase. Determination of selective isotope effects in the dehydrogenation of butyryl-CoA. *Eur. J. Biochem.* **160**, 109–115
6. Kim, J.-J.P., Wang, M., and Paschke, R. (1993) Crystal structures of medium-chain acyl-CoA dehydrogenase from pig liver mitochondria with and without substrate. *Proc. Natl. Acad. Sci. USA* **90**, 7523–7527
7. Massey, V. and Ghisla, S. (1974) Role of charge-transfer interactions in flavoprotein catalysis. *Ann. N.Y. Acad. Sci.* **227**, 446–465
8. Nishina, Y., Sato, K., Shiga, K., Fujii, S., Kuroda, K., and Miura, R. (1992) Resonance Raman study on complexes of medium-chain acyl-CoA dehydrogenase. *J. Biochem.* **111**, 699–706
9. Ikeda, Y., Okamura-Ikeda, K., and Tanaka, K. (1985) Spectroscopic analysis of the interaction of rat liver short-chain, medium-chain, and long-chain acyl coenzyme A dehydrogenases with acyl coenzyme A substrates. *Biochemistry* **24**, 7192–7199
10. Trievel, R.C., Wang, R., Anderson, V.E., and Thorpe, C. (1995) Role of the carbonyl group in thioester chain length recognition by the medium chain acyl-CoA dehydrogenase. *Biochemistry* **34**, 8597–8605
11. Lau, S.-M., Brantley, R.K., and Thorpe, C. (1988) The reductive half-reaction in acyl-CoA dehydrogenase from pig kidney: Studies with thiaoctanoyl-CoA and oxaoctanoyl-CoA analogues. *Biochemistry* **27**, 5089–5095
12. Tamaoki, H., Setoyama, C., Miura, R., Hazekawa, I., Nishina, Y., and Shiga, K. (1997) Spectroscopic studies of rat liver acyl-CoA oxidase with reference to recognition and activation of substrate. *J. Biochem.* **121**, 1139–1146
13. Gorelick, R.J., Mizzer, J.P., and Thorpe, C. (1982) Purification and properties of electron-transferring protein from pig kidney. *Biochemistry* **21**, 6936–6942
14. Lau, S.-M., Powell, P., Buettner, H., Ghisla, S., and Thorpe, C. (1986) Medium-chain acyl coenzyme A dehydrogenase from pig kidney has intrinsic enoyl coenzyme A hydratase activity. *Biochemistry* **25**, 4184–4189
15. Thorpe, C., Matthews, R.G., and Williams, C.H., Jr. (1979) Acyl-coenzyme A dehydrogenase from pig kidney. Purification and properties. *Biochemistry* **18**, 331–337
16. Uyeda, Y. and Reid, E.E. (1920) A sulfide acid or the butyl ether of thioglycolic acid. *J. Am. Chem. Soc.* **42**, 2385–2389
17. Kawaguchi, A., Yoshimura, T., and Okuda, S. (1981) A new method for the preparation of acyl-CoA thioesters. *J. Biochem.* **89**, 337–339
18. Stadtman, E.R. (1957) Preparation and assay of acyl coenzyme A and other thiol esters; Use of hydroxylamine in *Methods in Enzymology* (Colowick, S.P. and Kaplan, N.O., eds.) Vol. 3, pp. 931–941, Academic Press, New York
19. Bowman, W.D. and Spiro, T.G. (1981) Normal mode analysis of lumiflavin and interpretation of resonance Raman spectra of flavoproteins. *Biochemistry* **20**, 3313–3318
20. Abe, M. and Kyogoku, Y. (1987) Vibrational analysis of flavin derivatives: Normal coordinate treatments of lumiflavin. *Spectrochim. Acta* **43A**, 1027–1037
21. D'Ordine, R.L., Tonge, P.J., Carey, P.R., and Anderson, V.E. (1994) Electronic rearrangement induced by substrate analog binding to the enoyl-CoA hydratase active site: Evidence for substrate activation. *Biochemistry* **33**, 12635–12643
22. Kumar, N.R. and Srivastava, D.K. (1995) Facile and restricted pathways for the dissociation of octenoyl-CoA from the medium-chain fatty acyl-CoA dehydrogenase (MCAD)-$FADH_2$-octenoyl-CoA charge-transfer complex: Energetics and mechanism of suppression of the enzyme's oxidase activity. *Biochemistry* **34**, 9434–9443
23. Hazekawa, I., Nishina, Y., Sato, K., Shichiri, M., and Shiga, K. (1995) Substrate activating mechanism of short-chain acyl-CoA, medium-chain acyl-CoA, long-chain acyl-CoA, and isovaleryl-CoA dehydrogenases from bovine liver: A resonance Raman study on the 3-ketoacyl-CoA complexes. *J. Biochem.* **118**, 900–910
24. Miura, R., Nishina, Y., Fujii, S., and Shiga, K. (1996) ^{13}C-NMR study on the interaction of medium-chain acyl-CoA dehydrogenase with acetoacetyl-CoA. *J. Biochem.* **119**, 512–519
25. Kim, J.-J.P., Wang, M., Djordjevic, S., and Paschke, R. (1992) The three dimensional structure of acyl-CoA dehydrogenases in *New Developments in Fatty Acid Oxidation* (Coates, P.M. and Tanaka, K., eds.) pp. 111–126, Wiley-Liss, New York
26. Thorpe, C. and Kim, J.-J.P. (1995) Structure and mechanism of action of the acyl-CoA dehydrogenases. *FASEB J.* **9**, 718–725
27. Ghisla, S., Engst, S., Moll, M., Bross, P., Strauss, A.W., and

Downloaded from http://jb.oxfordjournals.org/ at Changhua Christian Hospital on October 1, 2012

Kim, J.-J.P. (1992) α,β-Dehydrogenation by acyl-CoA dehydrogenases: Role of functional groups at the active center in *New Developments in Fatty Acid Oxidation* (Coates, P.M. and Tanaka, K., eds.) pp. 127-142, Wiley-Liss, New York
28. Vock, P., Engst, S., Eder, M., and Ghisla, S. (1998) Substrate activation by acyl-CoA dehydrogenases: Transition-state stabilization and p*K*s of involved functional groups. *Biochemistry* **37**, 1848-1860
29. Lee, H.-J.K., Wang, M., Paschke, R., Nandy, A., Ghisla, S., and Kim, J.-J.P. (1996) Crystal structures of the wild type and the Glu376Gly/Thr255Glu mutant of human medium-chain acyl-CoA dehydrogenase: Influence of the location of the catalytic base on substrate specificity. *Biochemistry* **35**, 12412-12420
30. Nishina, Y., Sato, K., Hazekawa, I., and Shiga, K. (1995) Structural modulation of 2-enoyl-CoA bound to reduced acyl-CoA dehydrogenases: A resonance Raman study of a catalytic intermediate. *J. Biochem.* **117**, 800-808
31. Nandy, A., Kieweg, V., Kräutle, F.-G., Vock, P., Küchler, B., Bross, P., Kim, J.-J.P., Rasched, I., and Ghisla, S. (1996) Medium-long-chain chimeric human acyl-CoA dehydrogenase: Medium-chain enzyme with the active center base arrangement of long-chain acyl-CoA dehydrogenase. *Biochemistry* **35**, 12402-12411
32. Srivastava, D.K., Wang, S., and Peterson, K.L. (1997) Isothermal titration microcalorimetric studies for the binding of octenoyl-CoA to medium chain acyl-CoA dehydrogenase. *Biochemistry* **36**, 6359-6366
33. Rudik, I., Ghisla, S., and Thorpe, C. (1998) Protonic equilibria in the reductive half-reaction of the medium-chain acyl-CoA dehydrogenase. *Biochemistry* **37**, 8437-8445
34. Nakamura, H. (1996) Roles of electrostatic interaction in proteins. *Q. Rev. Biophys.* **29**, 1-90
35. Srivastava, D.K. and Peterson, K.L. (1998) Discriminatory influence of Glu-376→Asp mutation in medium-chain acyl-CoA dehydrogenase on the binding of selected CoA-ligands: Spectroscopic, thermodynamic, kinetic, and model building studies. *Biochemistry* **37**, 8446-8456
36. Kraulis, P.J. (1991) MOLSCRIPT: A program to produce both detailed and schematic plots of protein structures. *J. Appl. Crystallogr.* **24**, 946-950
37. McDonald, I.K. and Thornton, J.M. (1994) Satisfying hydrogen bonding potential in proteins. *J. Mol. Biol.* **238**, 777-793

Downloaded from http://jb.oxfordjournals.org/ at Changhua Christian Hospital on October 1, 2012